Deep Eutectic Solvent-Water Solvated Synthesis of Tungsten Oxide Nanoparticles with Photochromic and Antimicrobial Properties

Adetola Abiola Ajayi*, Olayinka Oderinde*, Sodiq Olalekan Ogunbayo, Olubunmi Ayoni Ogundiran, Adeola Roseline Olawuyi, Adebobola Ololade Agbeja

Editor's note: Photochromic and antimicrobial smart coatings hold great potential for advancements in modern applications, such as anti-UV photochromic contact lenses and bionic artificial skin. Ajayi et al. utilized deep eutectic solvents as a sustainable and adaptable medium for synthesizing tungsten oxide (WO_3) nanoparticles through an eco-friendly, low-temperature method. Optical analyses of the produced samples demonstrated strong UV absorption and a rapid, reversible photochromic transition occurring within just five seconds of UV exposure. Furthermore, antimicrobial tests indicated a dose-dependent bactericidal effect of the synthesized WO_3 nanoparticles against *Escherichia coli* and *Staphylococcus aureus*.

doi: 10.22034/jams.2025.210152

How to cite: A.A. Ajayi et al. *Journal of Applied Material Science*, **2025**, *1*, 210152.

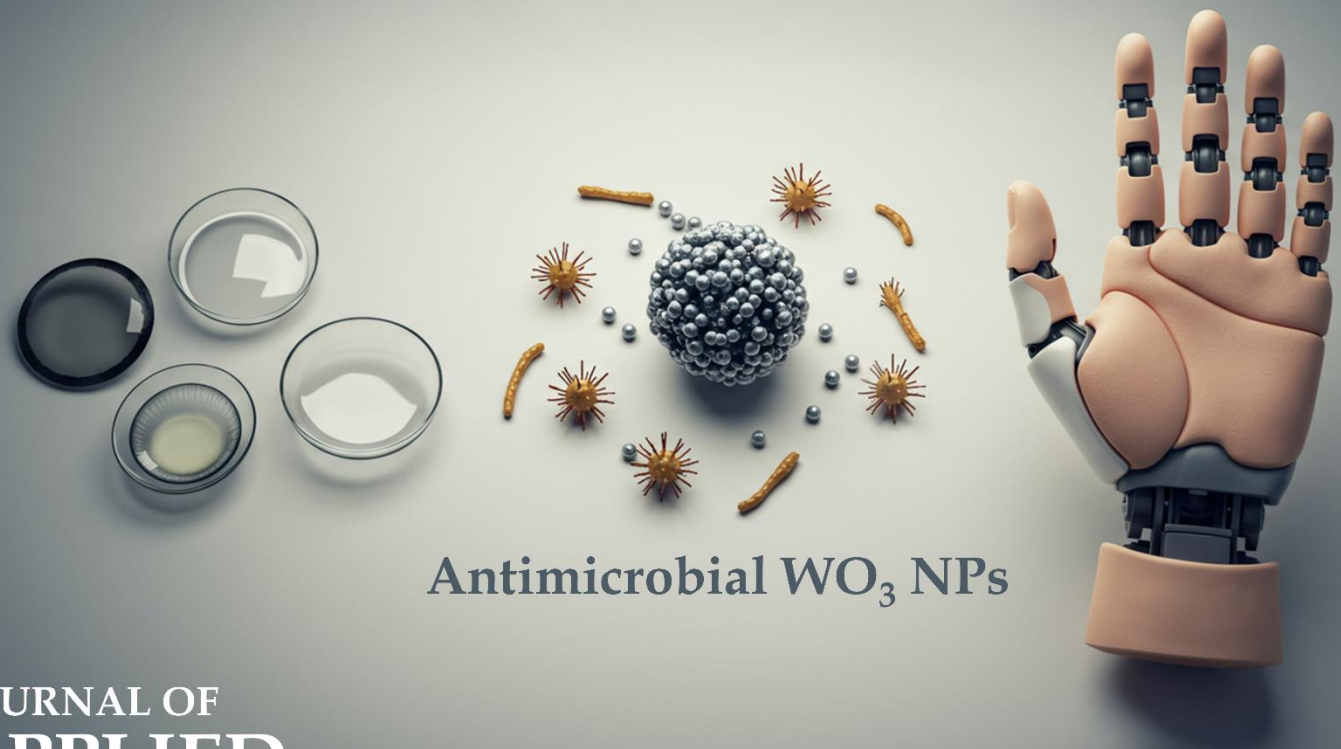

JOURNAL OF
APPLIED
MATERIAL
SCIENCE
jams.hsu.ac.ir

Journal of Applied Material Science **2025**, *1*, 210152
How to cite: A.A. Ajayi et al., *Journal of Applied Material Science*, **2025**, *1*, 210152.
Journal homepage: **jams.hsu.ac.ir**

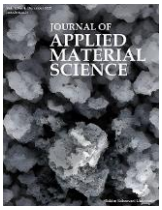

Original Research

Deep Eutectic Solvent-Water Solvated Synthesis of Tungsten Oxide Nanoparticles with Photochromic and Antimicrobial Properties

Adetola Abiola Ajayi [a,b,*], Olayinka Oderinde [a,c,*], Sodiq Olalekan Ogunbayo [a], Olubunmi Ayoni Ogundiran [d], Adeola Roseline Olawuyi [a], Adebobola Ololade Agbeja [e]

[a] *Department of Chemistry, Faculty of Natural and Applied Sciences, Lead City University, Ibadan, Nigeria*

[b] *Department of Science Laboratory Technology, School of Pure and Applied Sciences, Federal Polytechnic, PMB 50, Ilaro, Nigeria*

[c] *Department of Chemistry, Nile University of Nigeria, Plot 681, Cadastral Zone C-OO, Research & Institution Area, Jabi Airport Bypass, Abuja, FCT 900001, Nigeria*

[d] *Department of Chemical Sciences, Faculty of Sciences, Taraba State University, PMB 1167, Jalingo, Nigeria*

[e] *Department of Sustainable Forest Management, Forestry Research Institute of Nigeria, PMB 5054, Ibadan, Nigeria*

Abstract

Deep eutectic solvents (DESs) provide sustainable, tunable media for nanomaterial synthesis. In this work, tungsten oxide (WO_3) nanoparticles were prepared via a low-temperature green route using DES (choline chloride:ethylene glycol, 1:2) with varying water fractions to enhance solubility and reaction kinetics. Comprehensive characterization by FTIR, XRD, UV-Vis, SEM, and EDX confirmed the successful formation of WO_3 nanostructures with tunable crystallinity, morphology, and surface chemistry. FTIR spectra revealed distinct O-W-O/W-OH vibrational modes, while XRD identified monoclinic crystalline phases. SEM analysis demonstrated a morphology shift from irregular aggregates to sponge-like structures with increasing water content. Optical studies showed strong UV absorption (250-373 nm) and a rapid, reversible photochromic transition from transparent to blue within 5 s of UV exposure, fading back within 20 min under ambient conditions. Antimicrobial assays revealed dose-dependent bactericidal activity against *Escherichia coli* and *Staphylococcus aureus*, attributed to reactive oxygen species generation and oxygen-vacancy-mediated redox cycling, with the T1-D90W10 sample exhibiting the highest inhibition. This work establishes DES-water systems as versatile green platforms for fabricating multifunctional WO_3 Nanoparticles with synergistic photochromic and antimicrobial properties.

Keywords: Deep eutectic solvents; Tungsten oxide nanoparticles; Photochromic; Antimicrobial properties.

* Corresponding authors.
Email addresses: adetola.ajayi@federalpolyilaro.edu.ng (A.A. Ajayi), yinkaoderinde@yahoo.com (O. Oderinde)

Received 21 September 2025
Revised 4 October 2025
Accepted 14 October 2025
Available online 16 October 2025

https://doi.org/10.22034/jams.2025.210152

1. Introduction

Semiconducting metal oxides (SMOs) are increasingly recognized as multifunctional materials with applications spanning energy conversion, photocatalysis, smart coatings, and environmental remediation [1]. Their chemical robustness, tunable electronic structures, and strong light-matter interactions provide a solid foundation for developing next-generation functional materials [2]. Beyond these well-established uses, semiconducting metal oxides have also demonstrated promising antibacterial properties, positioning them as alternatives to traditional antimicrobial agents in biomedical and environmental settings.

Among these SMOs, tungsten trioxide (WO_3) has sparked notable interest as a result of its desirable qualities, including low toxicity, rich oxygen vacancy chemistry, and exhibiting a bandgap estimated at 2.6-3.0 eV, which enables visible-light responsiveness [1-3]. This optical activity not only underpins its photochromic behavior, where reversible color changes occur under light irradiation, but also supports the generation of reactive oxygen species (ROS) capable of disrupting bacterial membranes and metabolic functions [4].

Compared with conventional organic antibacterial compounds, WO_3-based nanostructures offer higher stability, extended durability, and broad-spectrum antimicrobial action [5]. Nevertheless, progress in the development of WO_3 nanomaterials that combine photochromic response with antibacterial activity has been limited, and much of the current research relies on synthesis methods such as electrospinning, which can be energy-intensive, high-cost of production, and less environmentally sustainable [6].

To address these challenges, DESs have arisen as attractive green media for nanomaterial fabrication, usually obtained by hydrogen-bond association between a salt and a hydrogen-bond donor.

DESs provide advantages such as low vapor pressure, tunable composition, and the ability to direct nanostructure formation [6, 7]. Importantly, the incorporation of water into DESs significantly modifies their physicochemical properties by lowering viscosity, enhancing ion mobility, and facilitating more uniform particle nucleation and growth. This DES-water medium thus provides a versatile platform for tailoring nanoscale morphology and functionality [8]. Furthermore, the use of DES-water systems in nanomaterial synthesis aligns with the growing emphasis on sustainable and low-energy processing routes, enabling scalable fabrication of WO_3 nanostructures with controlled features.

Adjusting the water content in DES serves as a tunable parameter that influences morphology, crystallinity, and surface activity, which in turn can optimize photocatalytic and antibacterial performance under visible light. Such flexibility highlights DES-assisted synthesis as a promising route for the development of multifunctional WO_3-based nanomaterials with industrial and biomedical relevance [9].

In the present study, WO_3 nanoparticles were synthesized using a DES-water co-solvent system as a structure-directing medium. The as-prepared WO_3 nanoparticles were systematically characterized for their morphological and structural properties, while their photochromic response and antibacterial activity were evaluated to highlight the multifunctional potential of DES-assisted synthesis routes.

2. Experimental

2.1. Materials

Analytical-grade reagents of high purity were used throughout the synthesis. Sodium tungstate dihydrate ($Na_2WO_4 \cdot 2H_2O$, 98.5%) was supplied by Shanghai Yuanye BioTech Co. Ltd. Choline chloride ($C_5H_{14}ClNO$, 98.0%) was obtained from Eastman Chemical Co. Ltd, while ethylene glycol ($C_2H_6O_2$, 99.0%), Ethanol (C_2H_5OH, 99.8%) and Glacial acetic acid (CH_3COOH, 99.5%) were purchased from Dow Chemical, USA. The bacterial strains *Escherichia coli* and *Staphylococcus aureus* were sourced from Thermo Fisher Scientific (USA).

2.2. Preparation of Ethaline (DES) Solution

Ethaline was obtained by mixing choline chloride (1 mol) with ethylene glycol (2 mol) and heating the mixture at 80 °C under continuous stirring for 60 min until a homogeneous, clear liquid was obtained. The resultant deep eutectic solvent was subsequently allowed to cool at room temperature before use [9].

2.3. Preparation of Tungsten Oxide Nanoparticles

An appropriate quantity (1 g) of sodium tungstate dihydrate was added separately into DES/water

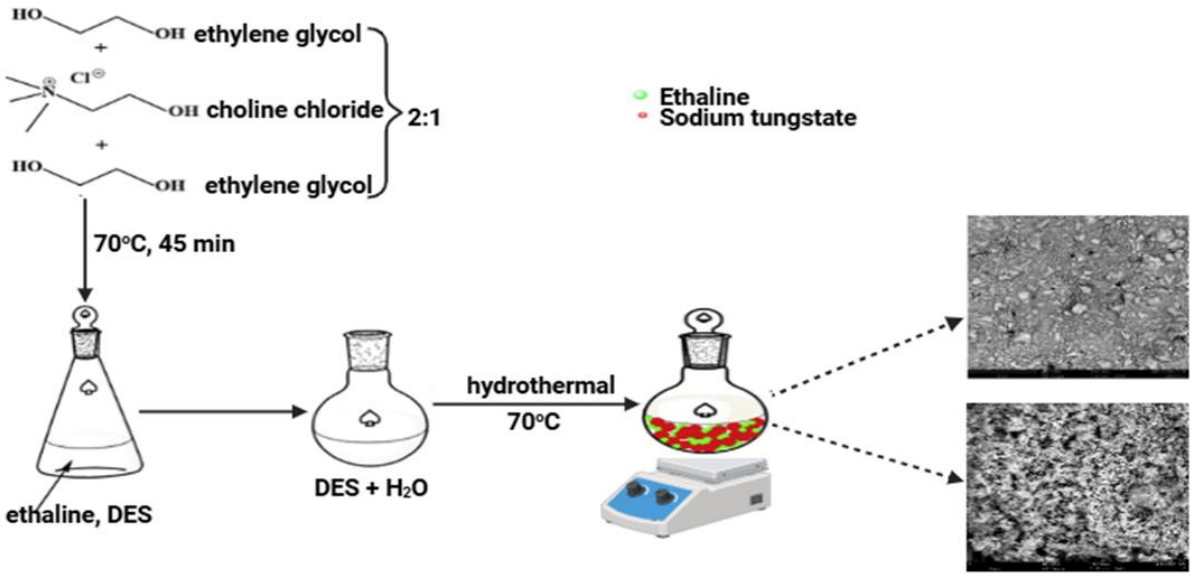

Figure 1. Schematic illustration showing the preparation and morphological transformation of the WO_3-NPs.

mixtures with different volume ratios: 90% DES/10% water (denoted as T1-D90W10), 80% DES/20% water (T1-D80W20), and 70% DES/30% water (T1-D70W30). Each mixture was heated to 70 °C on a magnetic stirrer hot plate under constant stirring for 30 min. Subsequently, 5 mL of glacial acetic acid ($C_2H_4O_2$) was added dropwise while stirring, and the reaction mixture was further stirred for 120 min. After cooling to room temperature, the suspensions were centrifuged at 5000 rpm for 20 min. The obtained precipitates were rinsed three times with ethanol to remove residual impurities, followed by drying in a hot-air oven at 80 °C for 12 h to yield tungsten oxide nanoparticles (Figure 1).

2.4. Measurements

Fourier transform infrared (FT-IR) spectra were obtained using a Nicolet iS50 spectrometer (Thermo Fisher, USA) in the 4000-400 cm^{-1} range with KBr pellets. X-ray diffraction (XRD) patterns were recorded on a SmartLab SE diffractometer (Rigaku, Japan) using Cu Kα radiation (λ = 0.15418 nm, 40 kV, 40 mA) over 10°-70° (2θ). Morphology and elemental composition were examined by scanning electron microscope (SEM) (JSM-7900F, JEOL, Japan) equipped with EDX. Optical absorption was measured with a Cary 5000 UV-Vis-NIR spectrophotometer (Agilent, USA) from 200-800 nm. Photochromic response was evaluated under 365 nm Xe lamp irradiation (300 mW cm^{-2}, Newport, USA) at 15 cm, with bleaching monitored in a dark, oxygen-rich atmosphere.

2.5. Photochromic Activity of As-Prepared Tungsten Oxide Nanoparticle.

The photochromic behavior of as-prepared samples was examined by dissolving 0.025 g of each material in 2 mL of deionized DI water. The mixtures were shaken for a few minutes, after which 1 mL of the resulting solution was transferred into a hollow groove. The samples were then irradiated with a 3 W, 365 nm light source (Shenyu Aic, Suzhou, China) placed 5 cm away, under ambient conditions [10, 11].

2.6. Antibacterial Test

To test their antibacterial effects, T1-D90W10 and T1-D70W30 were examined against *Staphylococcus aureus* and *Escherichia coli* using the agar disk diffusion method. Amoxicillin (30 mg) was included as a standard reference drug. The bacteria were first grown in nutrient broth and then evenly spread onto agar plates. Small sterile discs, each loaded with 100, 200, or 400 mg of the samples, were placed on the plates and left to incubate at 37 °C for 24 hours. After incubation, the clear zones around the discs, showing where bacterial growth was prevented, were measured. Each experiment was repeated three times, and the results are shown as the average values with their standard errors [12].

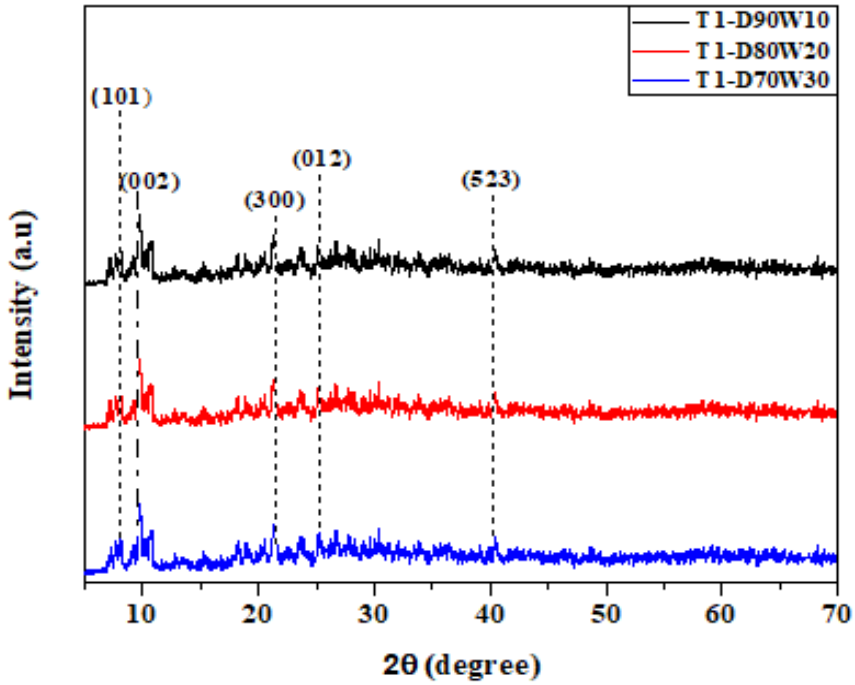

Figure 2. XRD patterns of as-prepared WO_3-NPs at different solvent volume ratios.

3. Results and discussion

3.1. XRD Analysis

Figure 2 shows XRD patterns of WO_3 nanoparticles synthesized using DES-water mixtures with different water contents. The diffraction peaks appear at the same position 8.12° (010), 10.66° (002), 21.34° (113), and 30.50° (130), corresponding to monoclinic tritungsten nonaoxide W_3O_9 (JPCDS Card 00-025-1496). However, the T1-D70W30 sample displays the most intense and well-defined crystallinity, while the T1-D90W10 sample presents broader and weaker peaks. This trend suggests that higher water content enhances crystallinity and promotes the growth of larger crystallite domains, whereas lower water levels result in smaller, less ordered particles. The improvement can be attributed to the ability of water to lower the viscosity of DES and accelerate the hydrolysis-condensation of the tungsten precursor, thereby supporting crystal development of WO_3 [13]. The crystallite sizes (Dc) of the samples were calculated using Scherrer's equation:

$$Dc = \frac{0.8\lambda}{\beta \cos\theta} \quad (1)$$

where Dc is the average crystallite diameter, λ is the wavelength of Cu Kα radiation (λ = 0.15418 nm), θ is the Bragg diffraction angle, and β is the full width at half maximum (FWHM) of the diffraction plane. Based on calculations from the intense diffraction peak, the crystallite sizes were determined to be 33.14nm, 33.59nm, and 33.89nm, respectively.

3.2. FTIR Analysis

Figure 3 shows FTIR spectra of as-prepared WO_3-NPs at different solvent volume ratios. In the fingerprint region (below 1000 cm^{-1}), the spectra clearly reveal the structural signatures of tungsten oxide nanoparticles. An intense signal around 898 cm^{-1} arises from the fundamental stretching vibrations of the metal-oxygen framework, while the peak at 776 cm^{-1} is linked to O-W-O bonds; both indicate the presence of WO_3 [14, 15]. Additional absorption features at 898 cm^{-1} and 979 cm^{-1} are linked to W-OH stretching vibrations [16]. The coexistence of O-W-O and W-OH modes in this region provides strong evidence for the successful formation of WO_3 nanoparticles [15, 16]. Moving to the mid-infrared region, distinct bands were also observed at 1469 cm^{-1} and 1081 cm^{-1}. The 1469 cm^{-1} peak corresponds to N-O stretching, pointing to traces of nitrate species possibly originating from the DES precursor, while bending

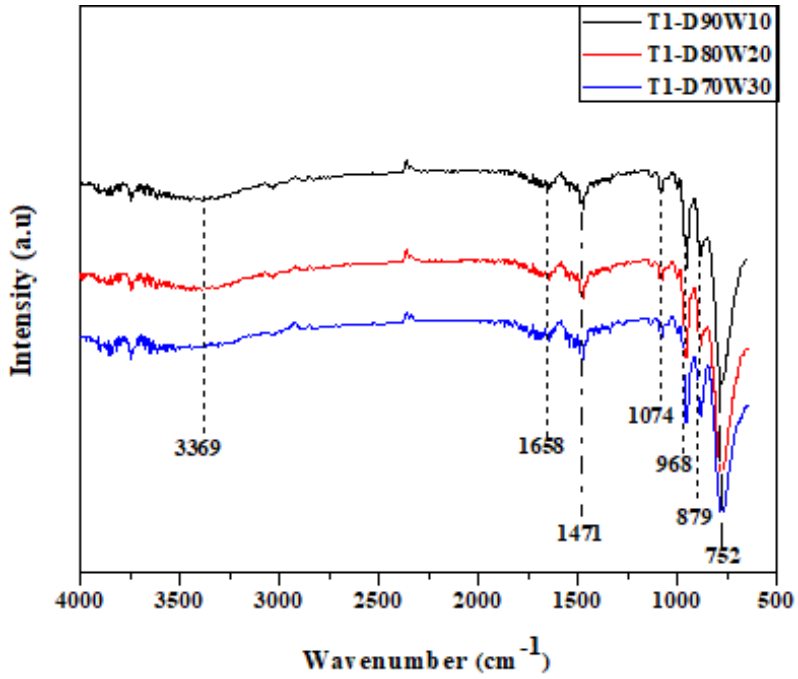

Figure 3. FTIR spectra of as-prepared WO_3-NPs at different solvent volume ratios.

vibrations of N-H in the same range indicate residual organic groups attached to the WO_3 surface [17].

At higher wavenumbers, a broad band near 3377 cm^{-1} represents O-H stretching, confirming the presence of hydroxyl groups from surface-adsorbed water or hydroxides. Similarly, a band at 1663 cm^{-1} is assigned to O-H bending, further highlighting the hydrated nature of the samples [17].

3.3. SEM Analysis

The SEM micrograph in Figure 4a reveals that the T1-D90W10 sample is composed of irregularly distributed, clustered crystals with non-uniform shapes. The particles appear highly aggregated, forming compact and coarse structures. This clustered morphology can be attributed to the limited solvation capacity and high viscosity of the DES medium in the absence of sufficient

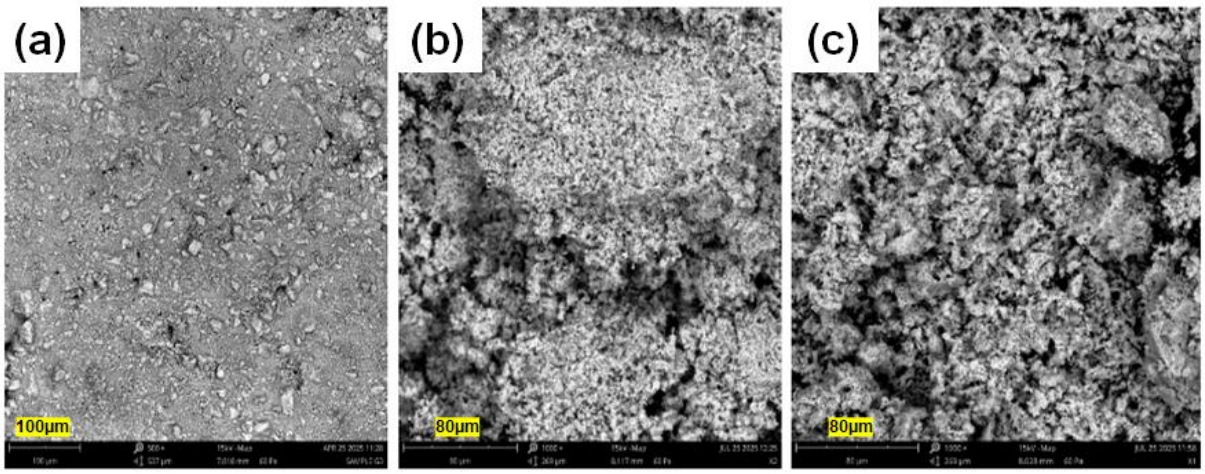

Figure 4. SEM images of the as-prepared WO_3-NPs: (a) T1-D90W10, (b) T1-D80W20, and (c) T1-D70W30.

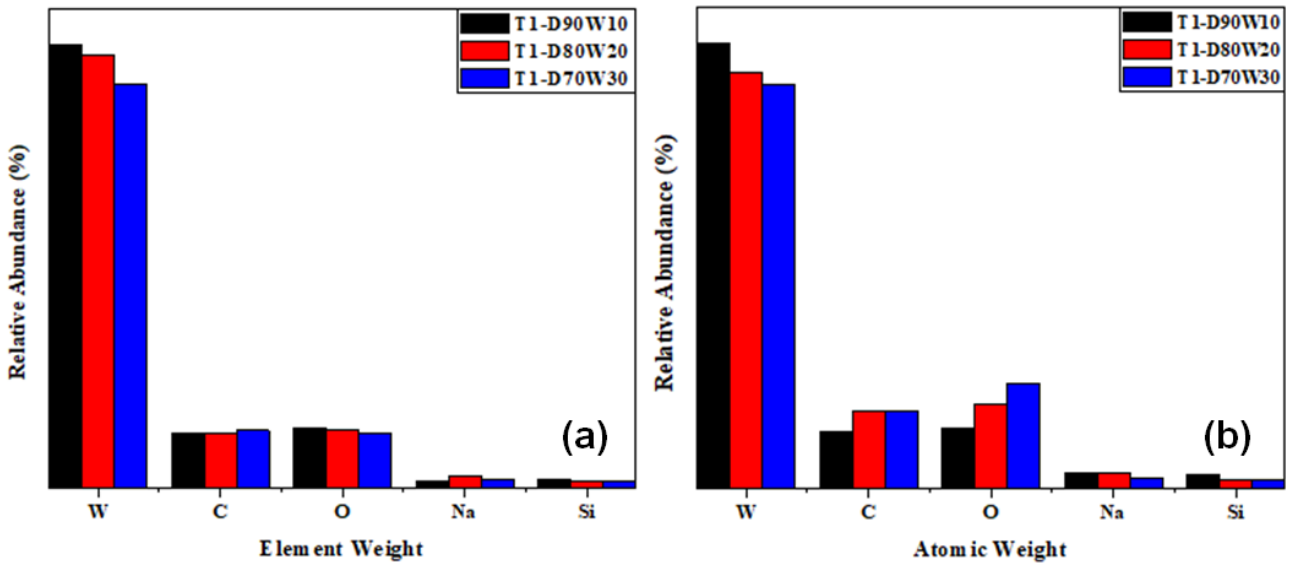

Figure 5. Variations in the relative elemental weight percent of the nanoparticles synthesized using different solvent volume ratios.

water, which restricts ion mobility and hinders uniform particle dispersion [18, 19].

Conversely, with increased water content (T1-D70W30), the morphology transforms into sponge-like formations, as shown in Figure 4c. This clearly demonstrates that the water concentration strongly influences the structural development and growth behavior of the composites. The observed morphological variation suggests that higher water content enhances solvation, thereby providing a more favorable reaction environment for uniform nucleation and controlled particle growth[12, 13]. Consequently, this results in a more refined and open microstructure within the DES-water-assisted system [10].

Energy Dispersive X-ray (EDX) analysis confirms the presence of tungsten (W), carbon (C), oxygen (O), sodium (Na), and chlorine (Cl) within the nanoparticles. Tungsten dominates the elemental composition, validating the formation of tungsten oxide (WO_3) as the principal crystalline phase [18, 19]. The high tungsten content suggests efficient incorporation of the metal precursor during synthesis, a factor critical for enhancing the nanoparticle's redox properties and antibacterial activity (Figure 5a and 5b).

3.4. UV Analysis

To assess the photochromic performance of the prepared samples, their light absorption behavior was examined using UV-Vis spectroscopy. As illustrated in Figure 6, the particles showed a strong and broad absorption response in the UV region, spanning 250-373 nm, with a peak threshold around 406 nm. This pronounced UV absorption can be linked not only to the influence of water but also to the presence of -OH and -NH groups originating from the deep eutectic solvent (DES) [17]. These groups, likely trapped within the aggregated particles, appear to facilitate the movement

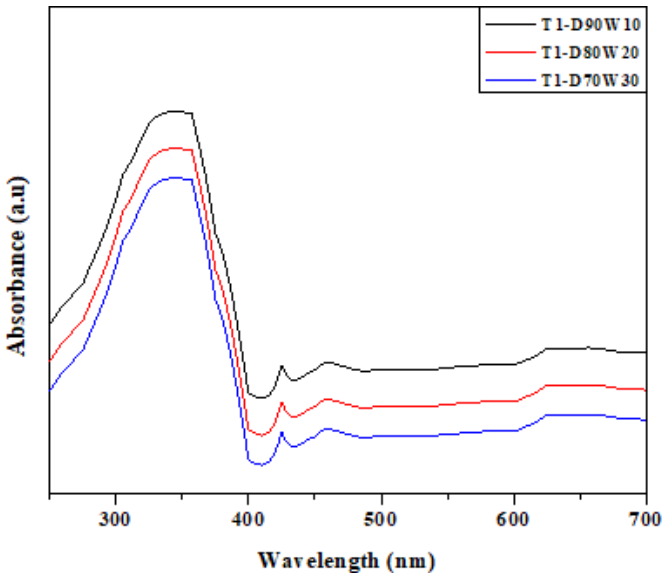

Figure 6. Absorbance characteristics of the as-synthesized WO_3-NPs at different solvent volume ratios.

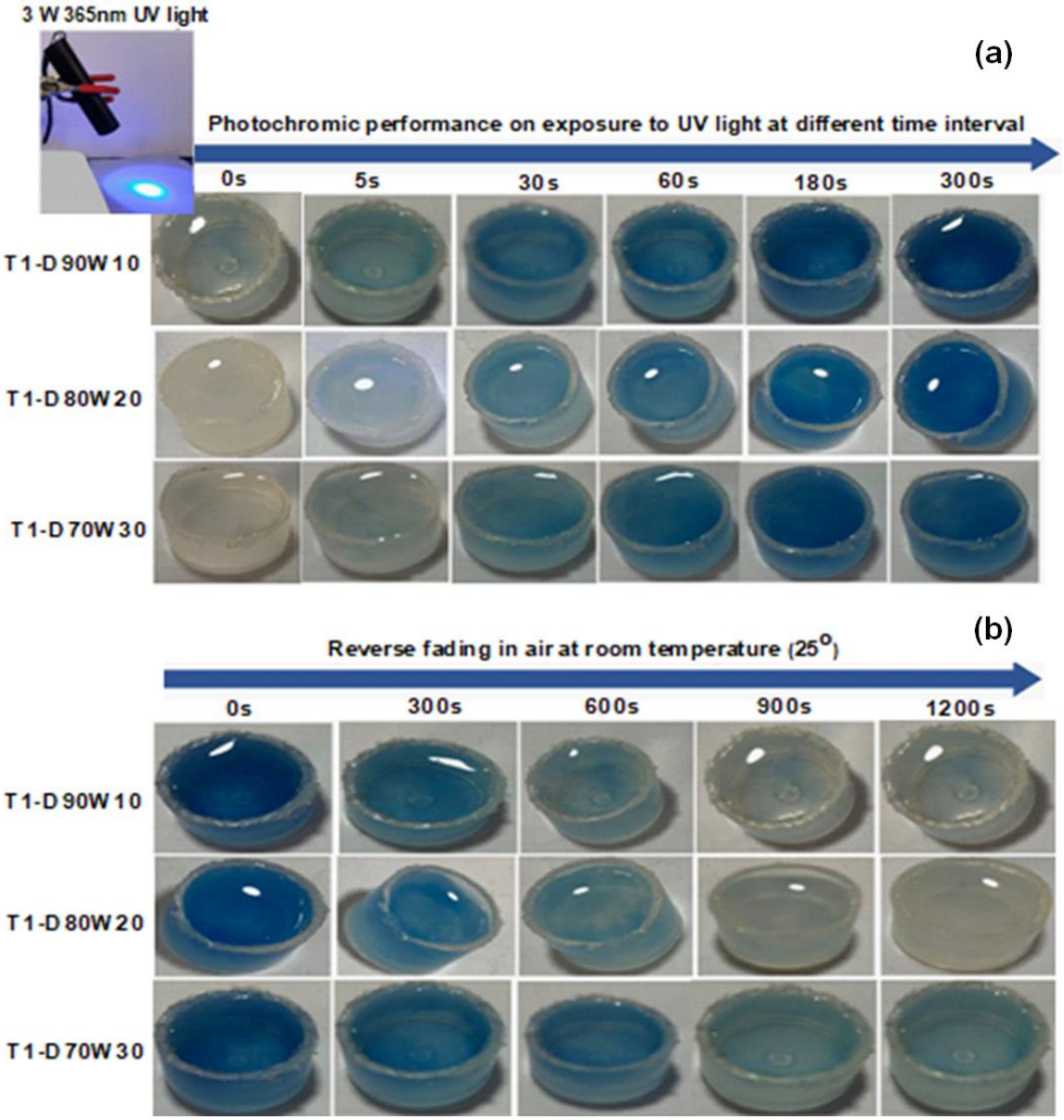

Figure 7. (a) Photochromic response and (b) reverse fading process of as-prepared WO_3 nanoparticles.

of photogenerated protons and electrons, thereby enhancing their transfer into the tungsten oxide semiconductor matrix (WO_3) [12]. In addition, the redshifted absorption edge observed in the samples indicates a slight narrowing of the bandgap, which favors visible-light responsiveness. Such modifications in optical properties highlight the synergistic role of DES-water interactions and functional groups in tailoring the electronic structure and improving the overall photochromic activity of WO_3 [16].

3.5. Photochromic Response and Reverse Fading Process

The photochromic behavior of the synthesized samples dispersed in deionized (DI) water was evaluated using a 3W UV lamp positioned 5 cm from the samples. As presented in Figure 7a, all samples showed a swift shift from transparency to a blue color within 5 seconds of irradiation, with the coloration gradually intensifying as the exposure time increased.

This optical transition is attributed to the participation of mobile ionic species (NH_4^+ and H^+) and water molecules, which facilitate photo-induced charge transfer processes. Ammonium and protonic species, originating from donor components such as ethylene glycol in the DES medium and water, are adsorbed onto the WO_3 surface and migrate through hydrated pathways, thereby accelerating the charge transport [17].

The observed coloration is governed by a reversible reduction of W^{6+} to W^{5+}, a mechanism that underpins the switching efficiency of WO_3 and highlights its suitability for photo-responsive applications, including smart coatings and optical sensors [18].

Among the tested materials, the T1-D70W30 sample displayed the most intense coloration. This behavior can be linked to the role of water, as hydrogen species are detached from hydrogen-donor molecules (the ethylene glycol component of the DES solvent) and from H_2O, subsequently becoming adsorbed onto the surface of the metal oxides through specialized water-mediated pathways. Under irradiation, this process promotes hydrogen spillover, which facilitates the development of photochromic systems with enhanced sensitivity [19]. The bleaching process, as shown in Figure 7b, occurred gradually in open air. The T1-D70W30 sample required approximately 1200 s for full fading, whereas the T1-D90W10 and T1-D80W20 dispersions recovered more rapidly. This accelerated recovery at lower water contents is attributed to enhanced re-oxidation of W^{5+} to W^{6+} by ambient oxygen, coupled with faster electron-hole recombination dynamics [15, 16]. Collectively, these results highlight the critical role of water in modulating proton availability, charge transport pathways, and ultimately the balance between coloration depth and recovery speed [16].

3.6. Antibacterial Activity of As-Prepared Samples

The antimicrobial activity of the synthesized samples (T1-D90W10 and T1-D70W30), shown in Figure 8, was evaluated using the disc diffusion method to measure the zone of inhibition, while the microtube dilution method was employed to determine the Minimum Inhibitory Concentration (MIC) across varying concentrations. To ensure uniformity of the inoculum and achieve confluent microbial growth, a McFarland 0.5 turbidity standard was applied. At its highest tested concentration (400 mg/ml), the T1-D70W30 sample exhibited no inhibitory activity against *Staphylococcus aureus* (Gram-positive). However, the same sample produced moderate inhibition zones against *Escherichia coli* (Gram-negative) when compared to ciprofloxacin (positive control), indicating some degree of selective antibacterial activity.

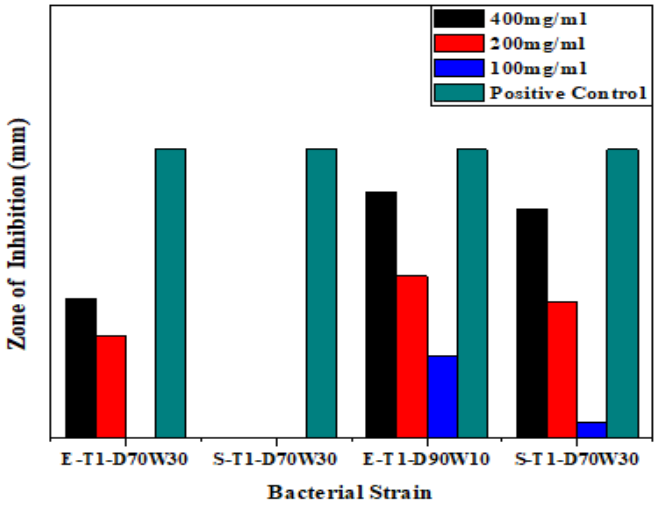

Figure 8. Antimicrobial activities of T1-D90W10 and T1-D70W30 composite against *S. aureus* and *E. coli*.

In contrast, the T1-D90W10 sample demonstrated stronger antimicrobial performance (Figure 8). It produced pronounced inhibition zones against *S. aureus* and moderate zones against *E. coli*, showing broader efficacy relative to ciprofloxacin [7]. However, the comparative results indicate that the T1-D90W10 sample was more effective than the T1-D70W30 sample in terms of inhibition zone diameter, MIC, and Minimum Bactericidal Concentration (MBC) [20, 21]. The reduced potency observed in the T1-D70W30 ml sample may be attributed to the higher water content, which could dilute active components, alter the chemical structure of Ethaline, or interfere with antimicrobial interactions at the bacterial membrane level. Such effects appear to vary with bacterial cell wall architecture, as differences were noted between Gram-positive (*S. aureus*) and Gram-negative (*E. coli*) strains [7, 22].

4. Conclusions

This work demonstrated the successful synthesis of reversible photochromic tungsten oxide nanoparticles via a simple, low-temperature, and environmentally friendly DES-water approach. Characterizations (FTIR,

XRD, UV-Vis, SEM-EDX) confirmed their controlled crystallinity, uniform distribution, and stable metal-oxygen bonding. The nanoparticles showed strong UV-Vis absorption, rapid coloration under UV irradiation, and reversible fading, highlighting their suitability for optical devices, sensors, and rewritable media. In addition, the WO_3 nanocomposites exhibited strong antimicrobial activity, effectively inhibiting both *Staphylococcus aureus* and *Escherichia coli* through synergistic ROS generation and oxygen vacancy-mediated redox cycling. This dual functionality, photochromism, and antimicrobial performance demonstrate the potential of DES-water synthesis as a sustainable platform for developing advanced nanomaterials with applications in healthcare, water purification, food safety, and protective equipment. The study provides new insights into how DES-water interactions influence nanoparticle functionality, offering a blueprint for tailoring material properties through green chemistry. Its findings also contribute to addressing global challenges of antimicrobial resistance while advancing multifunctional nanomaterials. Future work could explore the scalability and integration of these materials into practical devices and coatings.

Conflict of Interest

The authors declare no conflict of interest.

References

1. O. Ejeromedoghene, et al. Transparent and photochromic poly(hydroxyethyl acrylate–acrylamide)/WO_3 hydrogel with antibacterial properties against bacterial keratitis in contact lens. *Journal of Applied Polymer Science*, **2021**, *139*, 51815.
2. B. Cui, et al. Photochromic performance of hydrogel based on deep eutectic solvent induced water soluble Cu-doped WO3 hybrids with antibacterial property. *Journal of Photochemistry and Photobiology A: Chemistry*, **2023**, *435*, 114320.
3. Y.-H. Lu, et al. A facile green antisolvent approach to Cu²⁺-doped ZnO nanocrystals with visible-light-responsive photoactivities. *Nanoscale*, **2014**, *6*, 8796.
4. Y. Song, et al. Aqueous synthesis and photochromic study of Mo/W oxide hollow microspheres. *RSC Advances*, **2016**, *6*, 99898.
5. O.L. Pop, et al. Cerium Oxide Nanoparticles and Their Efficient Antibacterial Application In Vitro against Gram-Positive and Gram-Negative Pathogens. *Nanomaterials*, **2020**, *10*, 1614.
6. Y. Yao, et al. A Review on the Properties and Applications of WO3 Nanostructure−Based Optical and Electronic Devices. *Nanomaterials*, **2021**, *11*, 2136.
7. A. Salim and S. Sadhasivam. Biofabricated MoO3 nanoparticles for biomedical applications: Antibacterial efficacy, hemocompatibility, and wound healing properties. *Nano and Medical Materials*, **2023**, *3*, 73.
8. P.P. Tumkur, et al. Cerium Oxide Nanoparticles: Synthesis and Characterization for Biosafe Applications. *Nanomanufacturing*, **2021**, *1*, 176.
9. M. Nyoka, et al. Synthesis of Cerium Oxide Nanoparticles Using Various Methods: Implications for Biomedical Applications. *Nanomaterials*, **2020**, *10*, 242.
10. J. Gutpa, et al. PVD techniques proffering avenues for fabrication of porous tungsten oxide (WO3) thin films: A review. *Materials Science in Semiconductor Processing*, **2022**, *143*, 106534.
11. M. Aryafard, et al. Experimental and theoretical investigation of solvatochromic properties and ion solvation structure in DESs of reline, glyceline, ethaline and their mixtures with PEG 400. *Journal of Molecular Liquids*, **2019**, *284*, 59.
12. O. Oderinde, et al. Facile synthesis and study of the photochromic properties of deep eutectic solvent-templated cuboctahedral-WO3/MoO3 nanocomposites. *Superlattices and Microstructures*, **2019**, *125*, 103.
13. J. Gomez-Hermoso-de-Mendoza, et al. Flexible photochromic cellulose triacetate based bionanocomposites modified with sol-gel synthesized V2O5 nanoparticles. *Carbohydrate Polymers*, **2019**, *208*, 50.
14. Y. Chen, et al. Core-shell structured CsxWO3@ZnO with excellent stability and high performance on near-infrared shielding. *Ceramics International*, **2018**, *44*, 2738.
15. C. Dong, et al. A review on WO3 based gas sensors: Morphology control and enhanced sensing properties. *Journal of Alloys and Compounds*, **2020**, *820*, 153194.
16. L. Pan, Y. Shen, and Z. Li. Hydrothermal synthesis of WO3 films on the TiO2 substrates and their photochromic properties. *Materials Science in Semiconductor Processing*, **2015**, *40*, 479.
17. T.J. DeJournett and J.B. Spicer. The influence of oxygen on the microstructural, optical and photochromic properties of polymer-matrix, tungsten-oxide nanocomposite films. *Solar Energy Materials and Solar Cells*, **2014**, *120*, 102.
18. Y. Zhang, et al. Template-free to fabricate highly sensitive and selective acetone gas sensor based on WO3 microspheres. *Vacuum*, **2013**, *95*, 30.
19. V.S. Kavitha, et al. High quality, highly transparent Cu incorporated WO3 thin films suitable for blue LED application. *Vacuum*, **2020**, *172*, 109044.

20. V. Gopal, et al. Visible light photocatalytic decomposition of organic dye and biodegradation-resistant antibiotic pollutants using cerium-doped tungsten trioxide nanoparticles. *Research on Chemical Intermediates*, **2024**, *50*, 5097.

21. Y. Dai, et al. Application of natural deep eutectic solvents to the extraction of anthocyanins from Catharanthus roseus with high extractability and stability replacing conventional organic solvents. *Journal of Chromatography A*, **2016**, *1434*, 50.

22. A. Sharma, et al. Methods of preparation of metal-doped and hybrid tungsten oxide nanoparticles for anticancer, antibacterial, and biosensing applications. *Surfaces and Interfaces*, **2022**, *28*, 101641.